Fuel Processing Technology 293 (2026) 108630

Contents lists available at ScienceDirect

Fuel Processing Technology

journal homepage: www.elsevier.com/locate/fuproc

From food waste to kerosene: combined bio- and thermochemical processing via the intermediate product 2,3-BDO – a technical analysis

Felix Mendler [a,*], Steffen Voß [b], Martin Kaltschmitt [a]

[a] Institute of Environmental Technology and Energy Economics (IUE), Hamburg University of Technology (TUHH), Eißendorfer Straße 40, Hamburg, 21073, Germany
[b] Institute of Combustion Technology, German Aerospace Center (DLR), Am Haupttor, Bau 4310, Leuna, 06237, Germany

ARTICLE INFO

Keywords:
Sustainable aviation fuel
Process simulation
2,3-BDO
Technical evaluation
Carbon efficiency
Energy efficiency

ABSTRACT

In aviation, the most promising strategy for reducing greenhouse gas emissions is the use of sustainable aviation fuels (SAF). Biomass being a key feedstock poses specific challenges due to its limited availability and heterogeneous composition, highlighting the necessity for developing efficient and flexible conversion pathways for maximizing carbon and energy utilization. Given that integrated conversion pathways remain insufficiently explored, this study evaluates a novel, integrated process concept, utilizing food waste as the primary feedstock and combining biochemical conversion (consisting of dark fermentation, a microbial electrolysis cell and aerobic fermentation) with hydrothermal gasification to produce the intermediate 2,3-butanediol (2,3-BDO), followed by thermochemical conversion of 2,3-BDO to SAF. The overall process is modelled and simulated in Aspen Plus and evaluated in terms of overall carbon and energy efficiencies, supplemented by a sensitivity analysis of uncertain key parameters. The results show that the proposed pathway converts food waste into hydrocarbons with an overall carbon efficiency of 25.4% and an energy efficiency of 20.5%, of which 9.5% of the carbon and 7.6% of the energy are recovered as SAF. Additionally, the study identifies key parameters and strategies for potential process improvement, providing a quantitative basis for further process development.

1. Introduction

As the international community faces an increasing number of challenges due to the anthropogenic climate change, efforts to limit global warming at least to 2.0 °C above pre-industrial levels – as written in the Paris Agreement - must continue to intensify [1]. While some sectors have demonstrated measurable progress - particularly in the field of electricity generation, where renewables achieved a record 31.9% share of the global electricity generation in 2024 [2] - other sectors remain fundamentally difficult to defossilze and thus stay at a fairly low defossilization level. Within the transport sector, defossilization of aviation forms a particular challenge, because alternative propulsion options such as battery electric- or hydrogen-based systems cannot match the gravimetric and volumetric energy density, range performance and refuelling characteristics of hydrocarbon jet fuels for long-distance flights [3]. Furthermore, the existing global aircraft fleet and associated airport infrastructure are organized for kerosene as the main (and effectively the only) energy carrier. Consequently, there is a strong need for synthetically produced, drop-in liquid hydrocarbon fuels derived from renewable energy and/or waste resources that can be used within the existing fuel logistics and aircraft fleet; these fuels are commonly referred to as Sustainable Aviation Fuels (SAF) [4].

SAF can be produced from either biomass-derived carbon-based molecules or from biomass- or air-derived CO_2 in combination with hydrogen obtained either from biomass conversion or supplied as hydrogen via electrolysis using electricity from renewable sources of energy. Over the past decades, several SAF production pathways have been accepted by the American Society for Testing and Materials (ASTM) meeting the strict jet fuel specification [5].

Among these certified pathways, Hydroprocessed Esters and Fatty Acids (HEFA) has emerged as the dominant technology, accounting for roughly 90% of existing and announced global SAF production capacity due to its high technological maturity and ability to leverage existing refinery infrastructure [6]. However, HEFA relies on lipid feedstocks

Abbreviations: 2,3-BDO, 2,3-butanediol; ASTM, American Society for Testing and Materials; *C.nec.*, *Cupriavidus Necator*; HC, Hydrocarbon; EU, European Union; HEFA, Hydroprocessed esters and fatty acids; HHV, Higher heating value; LLE, Liquid liquid extraction; MEC, Microbial electrolysis cell; MEK, Methyl ethyl ketone; SAF, Sustainable aviation fuel.

* Corresponding author.
E-mail address: felix.mendler@tuhh.de (F. Mendler).

https://doi.org/10.1016/j.fuproc.2026.108630
Received 3 August 2026; Received in revised form 16 October 2026; Accepted 19 October 2026
Available online 21 October 2026
0378-3820/© 2026 The Authors. Published by Elsevier B.V. This is an open access article under the CC BY license (http://creativecommons.org/licenses/by/4.0/).
Open access funding enabled and organized by Projekt DEAL.

such as native vegetable oils, animal fats, and used cooking oils being characterized by constrained availability and competition with other sectors (e.g., the food sector) [5]. This feedstock limitation implies that HEFA alone cannot support the scale-up needed to align aviation with long-term climate targets [6]. This highlights the necessity of developing and deploying additional SAF production pathways to satisfy future demand and defossilization objectives.

Advanced biofuels must be produced from waste and residue streams to meet European Union (EU) criteria and avoid competition with food resources [7]. Food waste represents a major environmental, economic, and social challenge [8]. In the 27 member states of the EU in 2023, roughly 58.2 Mt of fresh food waste have been generated, with households accounting for more than half of the overall food waste generation [9]. To utilize this waste stream for SAF production, a technically and energetically optimal conversion route must be identified.

Among the various platform chemicals that can be converted to SAF, 2,3-butanediol (2,3-BDO) is an especially promising candidate. On the one hand, catalytic upgrading of 2,3-BDO to jet-range hydrocarbons via the same sequence of catalytic steps as a conventional alcohol-to-jet pathway (dehydration, oligomerization and hydrogenation) has been reported to achieve high carbon efficiencies [10]. On the other hand, 2,3-BDO is a multifunctional intermediate product with a wide range of applications that can be produced by fermentation using various bacterial strains and yeasts [11]. Additionally, acetoin, a key intermediate in the metabolic pathway for 2,3-BDO synthesis in most microorganisms [11], can be produced from volatile fatty acids – and particularly efficient from propionic acid – using a genetically engineered *Cupriavidus necator* (*C.nec.*) strain [12,13]. With further genetic modifications of the *C.nec.* strain, acetoin can be converted to 2,3-BDO, while additionally exploiting its autotrophic growth capacity enabling the conversion of CO_2 and H_2 into biomass and intermediate-products, including 2,3-BDO [14].

The present work focuses on a process combining biochemical routes for 2,3-BDO production from waste streams, in particular food waste, with thermochemical routes for SAF production. This concept aims to maximize overall carbon utilization while exploiting the energetic advantages of biological fermentation under mild operating conditions, while simultaneously enabling internal reuse of the effluent from the biological steps via a hydrothermal gasification unit. Hydrothermal gasification is a promising technology for the valorisation of wet organic residual streams by converting organic compounds into a gas mixture consisting mainly of CO, CO_2, H_2 and CH_4. The use of catalysts is a promising approach for reducing the required process temperature and enhancing product selectivity [15–17]. Therefore, with regard to the autotrophic growth capacity of *C.nec.*, catalytic hydrothermal gasification can be particularly suitable for recovering residual carbon and chemical energy from bioprocess effluents and redirecting it back to the bioprocess steps.

Previous studies have addressed individual segments of the investigated food waste to jet fuel value chain, including fermentative production of 2,3-BDO from bread waste [18] or gaseous substrates (CO_2 and H_2) [19], as well as the catalytic upgrading of 2,3-BDO to jet-fuel-range hydrocarbons [20,21]. However, no study has evaluated the complete integrated process chain of producing jet fuel from food waste using 2,3-BDO as an intermediate, including a catalytic hydrothermal gasification unit for effluent recovery and internal reuse.

The objective of the present study is to technically evaluate the novel SAF production process via the intermediate 2,3-BDO by quantifying its carbon and energy efficiencies and analysing how these performance indicators respond to fluctuations in uncertain process parameters.

2. Methodology

The following sections describe the methodological approach used to establish and evaluate the process. This includes an overview of the process design, its main design motivations and the conversion routes investigated; a description of the process modelling framework and overarching modelling assumptions; and an introduction to the key indicators of the technical analysis (i.e., carbon- and energy efficiency).

2.1. Process design

The process design is derived from the conceptual framework developed within the EU Horizon project BIOCTANE (project website: https://www.bioctane.eu/) investigating integrated pathways for producing sustainable aviation fuel. Due to the early development stage of most investigated reactor systems (technology readiness levels (TRL) of ca. TRL 1 to 3), the process remains in the basic research and laboratory scale phase. Consequently, the design aims to conceptually demonstrate process integration and evaluate technical performance rather than representing an industrial-scale configuration. Process parameters are based on experimental data generated within the BIOCTANE project's experimental work packages, supplemented by literature data when project data are unavailable.

The investigated conversion route from household food waste to kerosene is presented in Fig. 1. In the following subsections the process design is presented beginning with a description of the main feedstock, followed by a brief explanation of the conversion pathways to the intermediate-product 2,3-BDO, and concluding with the thermochemical conversion steps of 2,3-BDO to kerosene. Additionally, a catalytic hydrothermal gasification step is introduced to recover and reutilize the solid fraction produced during the bioconversion stages of the process. These recycling streams follow an internal recycling strategy, enabling inside the system boundaries the production of a gaseous intermediate that can be fed back to the bioconversion steps for 2,3-BDO production.

In the biochemical section, no external hydrogen supply is considered, reflecting the biological production constraints and self-contained stoichiometry of the fermentation routes. Hydrogen provision is considered only in the thermochemical conversion section, where hydrogen (considered as green hydrogen, produced via water electrolysis powered by electricity from renewable sources of energy) is required for hydro-processing and deoxygenation reactions.

2.1.1. Bioconversion steps – food waste to 2,3-BDO

In the first process section, a series of integrated bioconversion steps are carried out to convert food waste into high-purity 2,3-BDO through fermentation and subsequent purification. The block flow diagram of these bioconversion steps is shown in Fig. 2.

Main feedstock and pre-treatment. Against the background of the EU criteria for advanced biofuels and the large quantity of available food waste within the 27 member states of the EU [7,9], its utilization as a biogenic carbon source for SAF production seems to be particularly attractive. Therefore, a representative composition of average household food waste according to Table 1 is assumed as feedstock here.

Household food waste is processed before providing it as substrate to microorganisms inside the dark fermentation. The efficiency of the dark fermentation process (or anaerobic digestion process) is increased by reducing the particle size of food waste; i.e., the specific surface area is increased to improve the biodegradability of these waste material [23–25]. A mechanical pre-treatment is selected; various types of hammer, disk or ball mills are available for grinding such organic material [26].

Dark Fermentation. The mechanical pre-treated food waste is further processed via a mixed microbial anaerobic fermentation to produce a liquid fermentation broth with a high concentration of volatile fatty acids, with a particular focus on propionic acid production.

The use of a mixture of microorganisms within an anaerobic fermentation process is already well established. Although over 8500 biogas plants are operational only in Germany, anaerobic digestion still faces technical challenges, including unpleasant odours, leaks posing hazards to climate and local environment as well as the accumulation of inhibitors that can disrupt the process [27]. In recent years, research has

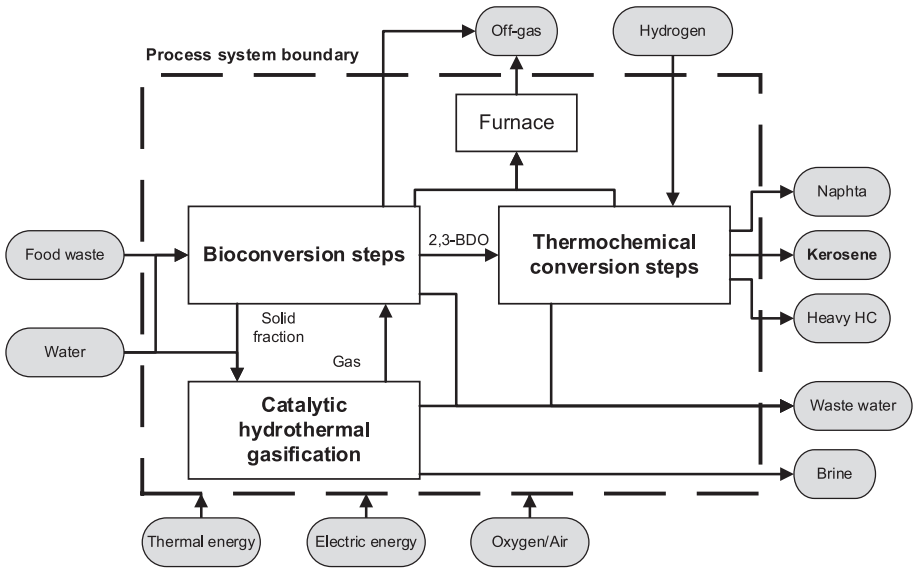


Fig. 1. Process overview (HC hydrocarbon).

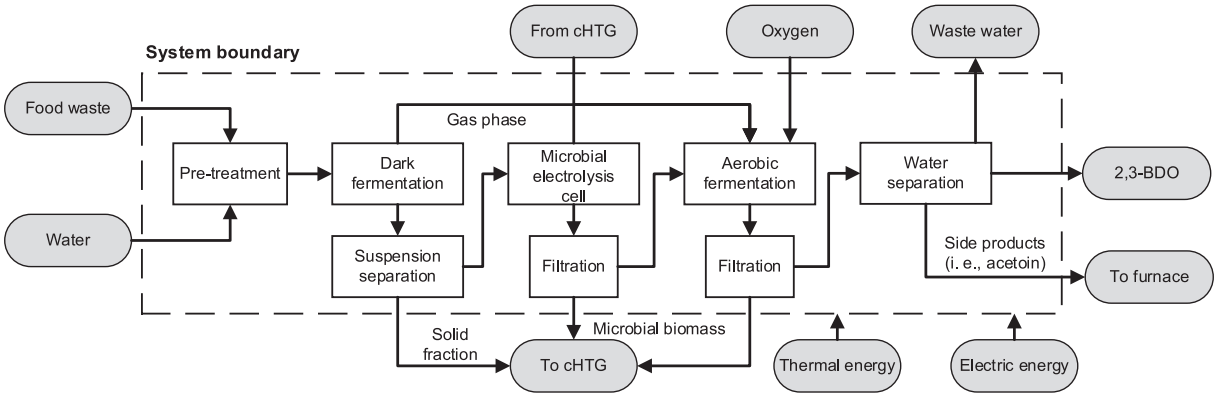


Fig. 2. Block flow diagram of the bioconversion process steps (cHTG Catalytic hydrothermal gasification).

Table 1
Assumed food waste composition [22].

Fresh matter food waste	Share in [wt%]
Water	76
Inorganic	2
Volatile Solids	22
Biochemical composition of the Volatile Solids	Share in [wt%]
Starch	48
Proteins	21
Lipids	15
Hemicellulose	7
Cellulose	6
Lignin	3

focused on alternative fermentation products to methane to improve the overall conversion efficiency and to develop a more robust process, as methanogenesis is a particularly slow and easily disrupted step in anaerobic digestion [28]. Therefore, an anaerobic fermentation toward a mixed production of volatile fatty acids, also often referred to as dark fermentation, is used as the first step of processing the pre-treated food waste. In addition to the liquid fermentation intermediate-products, a gaseous phase, consisting mainly of CO_2 and H_2, is provided. Additionally, after separation, a solid phase, containing microbial biomass and the undigested and indigestible parts of the food waste, is produced.

Dark fermentation has so far not progressed beyond pilot-scale applications and is predominantly investigated for biohydrogen production [29]; consequently, optimal operating conditions for a propionic-acid-rich fermentation remain a research topic. Depending on the applied conditions (e.g., pH, inoculum source, temperature, hydraulic retention time), different microbial communities are enriched during the biochemical degradation process, which in turn leads to distinct intermediate-product distribution [30].

Microbial electrolysis cell. The liquid phase leaving the dark fermentation step, now enriched in carboxylic acids, gets further processed in a microbial electrolysis cell (MEC). This step is introduced to obtain a metabolic profile enriched in propionic acid, as *C.nec*, the microorganism used in the downstream aerobic fermentation, performs particularly efficient when propionic acid is supplied as a substrate [12]. In the microbial electrolysis cell, acetic acid, which is the dominant carboxylic acid in the effluent coming from the dark fermentation step, can be selectively oxidized electrochemically by electroactive microorganisms (e.g., *Geobacter sulfurreducens* [31]), thereby lowering its concentration relative to the higher volatile fatty acids [32]. As a result of this electrochemical polishing, propionic acid, formerly the second most abundant carboxylic acid (under applied dark fermentation conditions), becomes the predominant acid in the liquid phase. After the microbial electrolysis cell, the formed microorganisms are separated by filtration, allowing the liquid to be considered microbially free and subsequently

fed to the aerobic fermentation.

A microbial electrolysis cell is conceptually similar to a conventional water electrolyser, consisting of an anode and a cathode compartment separated by a proton exchange membrane and connected via an external power supply [33]. The key difference to a water electrolyser is the presence of an anodic biofilm, which acts as a biocatalyst and oxidizes organic substrates (i.e., acetic acid) to CO_2 and protons instead of oxidizing water. The protons migrate through the proton exchange membrane and are reduced at the cathode together with electrons (supplied by the power source) to form H_2. Because organic compounds are oxidized rather than water, the required cell voltage is significantly lower compared with conventional water electrolysis, which translates into reduced electrical energy demand for hydrogen production in microbial electrolysis cells [34].

Aerobic fermentation. For the production of the intermediate chemical 2,3-BDO, an aerobic bioconversion step is applied. Using a genetically engineered strain of the aerobic, non-pathogenic bacteria *C. nec.* H16, 2,3-BDO can be produced. *C.nec.* can convert carboxylic acids – especially favouring propionic acid – into acetoin [12], a key predecessor in the 2,3-BDO biosynthesis [11]. In addition to this heterotrophic route based on carboxylic acids, an autotrophic pathway enables *C.nec.* to produce 2,3-BDO from a gaseous substrate consisting of CO_2 and H_2, with hydrogen serving as the electron donor [14].

Both pathways are implemented in the aerobic fermentation reactor, which can be configured with an internal membrane bundle that, on the one hand, enabling efficient CO_2/H_2 gas supply to the culture and, on the other hand, retains the bacterial cells within the reactor system [35]. To avoid the formation of an explosive O_2/H_2 gas mixture, oxygen is supplied via an additional aeration unit located at the bottom of the reactor. Again, the excess microorganisms are separated from the fermentation broth by filtration.

2,3-BDO purification. The purification of 2,3-BDO from the fermentation broth was designed as a multistage process to achieve an intermediate-product purity above 97 wt%. The process scheme comprises three main purification steps: membrane pre-concentration, liquid-liquid extraction, and multistage rectification.

In the first step, a reverse osmosis unit concentrates the dilute fermentation broth to ca. 10 wt% 2,3-BDO being the starting concentration reported for an effective liquid-liquid extraction [19,36,37]. This pre-concentration step primarily reduces water load for subsequent downstream operations and therefore enables a more efficient extraction performance.

The concentrated intermediate-stream is next subjected to liquid-liquid extraction (LLE) using decanol as the organic solvent. Decanol was selected due to its favourable properties – limited solubility in water and a boiling point sufficiently higher than that of 2,3-BDO, which facilitates downstream separation. Although decanol has not been extensively studied as an extraction solvent for 2,3-BDO, its physico-chemical properties and structural similarity to other long-chain alcohols which have been studied as extraction agents (e.g., hexanol, heptanol, oleyl alcohol) suggest good solvent selectivity [36,38].

The organic phase from the liquid-liquid extraction step undergoes a three-column rectification sequence. The first column recovers and recycles the decanol solvent. The second column removes residual water, and the third separates acetoin, a side-product of aerobic fermentation, which is used for energy recovery in the furnace. The final intermediate stream achieves a purity exceeding 97 wt% 2,3-BDO and a recovery rate above 88%.

2.1.2. Catalytic hydrothermal gasification

To utilize the undigested and indigestible parts of the food waste remaining after dark fermentation and to recover carbon losses associated with microbial growth inside the bioconversion steps, a catalytic hydrothermal gasification unit is integrated into the process. Under hydrothermal conditions, organic material is converted into a gaseous intermediate-product.

To achieve the supercritical state of water, elevated pressures (typically above 220 bar) and temperatures (around 375 °C or higher) are required [17]. Under these conditions, the solubility of inorganic salts decreases significantly, leading to the formation of a concentrated brine waste-stream that can be separated from the system, which could subsequently be used as a fertilizer [16,39].

In recent years, hydrothermal gasification has been developed and investigated primarily for methane production [16]. However, since methane cannot be digested by the *C.nec.* via the autotrophic pathway, a modified catalytic approach is investigated to shift the gas component distribution toward CO_2 and H_2.

A catalyst selective toward CO_2 and H_2 formation has been reported, consisting of platinum supported on γ-alumina. Although this study was conducted at laboratory scale using a uniform ethylene glycol feedstock, the reported carbon selectivity of 95% toward CO_2 has been adopted in the present work as a first assumption for the complex residue recycle-stream from the bioconversion step [17]. The applicability of this selectivity to the complex residue recycle-stream has not yet been experimentally validated and therefore represents an uncertainty of the present process assessment. To prevent catalyst deactivation, a sulphur trap is installed upstream of the catalyst bed to capture sulphur compounds, while nitrogen present in the feedstock is expected to form ammonia under hydrothermal conditions [16]. This configuration is illustrated as a block flow diagram in Fig. 3.

2.1.3. Thermochemical conversion steps – 2,3-BDO to kerosene

In the final process section, 2,3-BDO gets thermochemically converted into kerosene. Conventional fossil-based kerosene, obtained by distillation of crude oil, consists primarily of hydrocarbons with carbon chain lengths ranging from C_9 to C_{16} and a boiling range between 150 and 290 °C [40] (for the specifications for synthetic kerosene defined in the norm of the American Society for Testing and Materials (ASTM) ASTM D7566 and used to model kerosene in the process simulation, see Supplementary Material Table S9).

The conversion of 2,3-BDO into the target kerosene-range hydrocarbon mixture involves three key steps (dehydration, oligomerization, and hydrogenation) followed by separation of the hydrocarbons via distillation (i.e., fractionation), as illustrated in Fig. 4, thereby following the pathway of an alcohol-to-jet process already approved for ethanol and isobutanol under ASTM D7566 [5].

Dehydration. In the dehydration step, oxygen is removed from 2,3-butanediol (2,3-BDO) forming water and unsaturated C_4 components as main products, typically in the gas phase under a hydrogen atmosphere over solid acid catalysts (e.g., metal/zeolite systems) [41,42]. The selectivity toward different product types varies with the choice of the catalyst and the applied reaction conditions. Vapor-phase dehydration of 2,3-BDO is typically carried out at temperatures between 200 and 300 °C and at pressures ranging from approximately atmospheric pressure up to about 10 bar, depending on reactor design and process integration [42,43].

Here, data from a dehydration reaction system equipped with a CuO-ZSM catalyst are used, in which complete conversion of 2,3-BDO was reported, with a butene selectivity (Eq. (1)) exceeding 84 mol% (product distribution without water) [44].

$$C_4H_{10}O_2 + H_2 \rightarrow C_4H_8 + 2\,H_2O \quad (1)$$

Oligomerization. To obtain hydrocarbons in the kerosene-range, the short-chain alkenes (mainly butenes) formed after the dehydration of 2,3-BDO must undergo a chain-growth reaction. Depending on the reacting monomer and the reaction conditions, different degrees of oligomerization can be achieved. The oligomerization of a single alkene can be described by Eq. (2); however, mixtures of different short-chain alkenes can also be used as feedstock, which in both cases leads to a product mixture of alkenes with varying chain lengths [45–47]. For the formation of longer-chain hydrocarbons, elevated pressures in the magnitude of 20 to 40 bar and temperatures of about 100 to 400 °C are

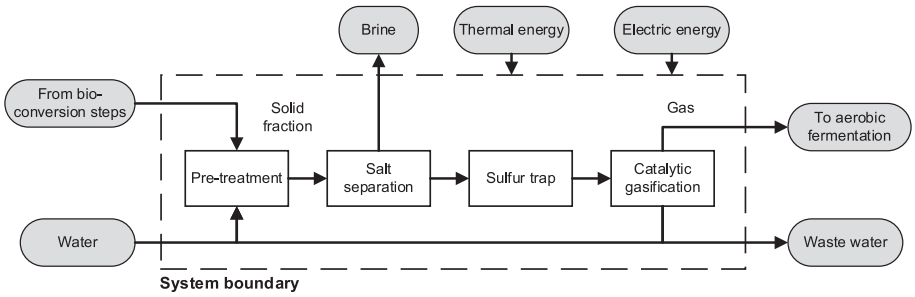


Fig. 3. Block flow diagram of the catalytic hydrothermal gasification.

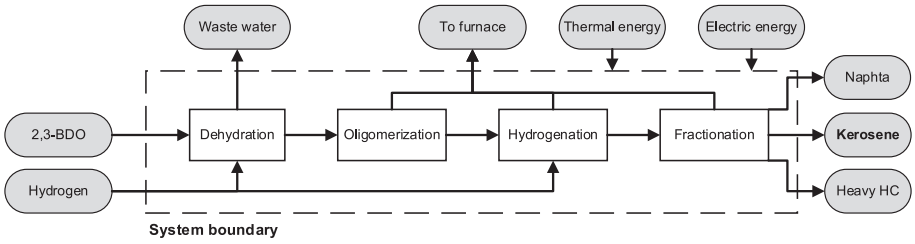


Fig. 4. Block flow diagram of the 2,3-BDO to kerosene conversion step.

typically required, largely independent of the implemented catalyst [46,48–50].

$$n\ C_xH_{2x} \rightarrow C_{nx}H_{2nx} \mid n \leq 2 \quad (2)$$

To describe the product spectrum obtained from the oligomerization reaction, the Anderson–Schulz–Flory distribution is applied as a mathematical model. This distribution has been widely used to represent product distributions in oligomerization reactions, most notably in Fischer-Tropsch synthesis using CO and H_2 as reactants [51–53], and has also been extended to systems involving longer reactants such as ethylene [50,54].

Hydrogenation. Hydrogenation is a well-established process that is already widely applied in the petroleum industry. During hydrogenation of alkenes, the C=C double bonds are saturated by the addition of hydrogen in the presence of a solid catalyst (such as Ni–W/alumina), resulting in the formation of the corresponding alkanes [55–57].

Fractionation. After obtaining the alkanes, the final step is to separate them into the corresponding fuel fractions (i.e., naphtha, kerosene, heavy alkanes). This separation step is also well established in the petroleum industry, where crude oil is distilled and fractionated into the respective fuel cuts. This process step ensures that the kerosene fraction meets the required boiling curve specifications outlined in ASTM D7566 [5].

2.2. Process modelling

The process is modelled in a steady-state flowsheet simulation using the process simulation software Aspen Plus [58] to establish a complete mass and energy balance across the overall process. Power inputs were treated as external utilities supplied to the respective units. To achieve optimal heat recovery and minimize the energy demand for heating and cooling from external sources, a pinch analysis is performed using Aspen Energy Analyzer [59] to identify optimal integration of the process heat streams.

Different property methods are applied along the process pathway. A detailed description of all stoichiometric reactions, operating conditions and thermodynamic models is provided in the Supplementary Information.

2.2.1. Data assumptions

Household food waste is assumed to correspond to the average European food waste composition after collection and impurity removal [22]. Particle size is reduced to 3 mm using a meat shredder, followed by dilution with water to the target substrate concentration and heating to 35 °C [60]. The dark fermentation is represented by a set of stoichiometric reactions for hydrolysis and acidogenesis of carbohydrates, lipids and proteins, with reaction rates calibrated to match experimentally observed volatile fatty acid and hydrogen yields (Table S1 – Supplementary Information). Generic components (triolein for lipids, gelatine for proteins, $C_5H_7NO_2$ for biomass) are used to represent complex substrates and microbial matter [61–70].

In the microbial electrolysis cell, only acetic acid is assumed to be electro-biochemically converted to hydrogen and CO_2 by *Geobacter sulfurreducens*, with an assumed overall acetic acid conversion rate of 0.8 and a fixed, literature-derived hydrogen recovery rate of 0.7. The electrical power input is determined based on the applied cell voltage, the number of electrons transferred in the electrochemical conversion of acetic acid, and the conversion rate of acetic acid. The waste heat released during the reaction is calculated as the difference between the supplied electrical work and the reaction enthalpy. Biomass formation is represented by an empirical formula, and complete biomass removal is assumed [32,33,71–76].

Aerobic fermentation is modelled via heterotrophic and autotrophic reactions converting volatile fatty acids and CO_2/H_2 to 2,3-butanediol (2,3-BDO), acetoin and biomass based on literature yields [12,14,19] (Table S3 – Supplementary Information); volatile fatty acids are fully converted in the heterotrophic stage, all microbial growth is assigned to heterotrophic stage, and fixed intermediate-product distributions and hydrogen consumption are assumed.

In catalytic hydrothermal gasification, all organics are first idealized as decomposed into their elemental forms at 420 °C and 270 bar. Inorganics are completely removed into a brine waste-stream via a salt separator, taking advantage of their low solubility under supercritical water conditions. Organic losses in the brine are represented by a single generic compound, and sulphur is captured separately in a dedicated sulphur trap. Gasification reactions are adjusted to achieve a target gas-phase carbon distribution of 95% CO_2, 4% CH_4 and 1% C_2H_6, assuming complete carbon gasification and complete conversion of nitrogen to NH_3 [16,17,39,77,78].

2,3-BDO purification combines reverse osmosis, LLE with decanol and a three-column distillation sequence. The LLE was modelled using an activity-coefficient-based approach, which has been reported as suitable for the extraction of 2,3-BDO using long-chain extraction systems such as heptanol [36]. In addition, its applicability to decanol-water extraction systems involving organic acids, including acetic and citric acid, has been reported [79,80]. The reverse osmosis membrane is characterized by fixed rejection factors per component [19,81] (Supplementary Information – Table S4), and the overall scheme achieves a 2,3-BDO purity of 97.4 wt% at 89.5% recovery.

Dehydration of 2,3-BDO at 250 °C and 1 bar yields mainly butene as dominant intermediate-product; reaction rates are adjusted to match reported dehydration-product distributions (Supplementary Information – Table S6), while hydrogen, water, and co-products are separated and hydrogen is fully recycled [44].

Oligomerization of C_2 to C_6 olefins at 225 °C and 30 bar is described by an Anderson-Schulz-Flory type chain growth model at 95% olefin conversion and fixed chain-growth probability factor $\alpha = 0.375$, targeting a high kerosene-range yield; unreacted light olefins are recycled with a 10% purge to the furnace [46,48–50].

Subsequent hydrogenation at 100 °C and 17 bar assumes complete conversion of olefins to paraffins with full hydrogen recycle and a 5% purge [57], followed by two distillation columns that define naphtha, kerosene (ASTM D7566) and heavier fractions.

2.2.2. Sensitive parameters

Due to the low technology readiness level (TRL) of several process steps and the limited availability of experimental data, key model parameters are subject to considerable uncertainty. Therefore, several parameters are investigated through a sensitivity analysis by systematically varying each parameter and rerunning the simulation for every increment. The results are used to highlight the influence of the investigated parameters on the overall process performance and to derive strategies for improving process efficiency.

2.3. Process performance evaluation

The carbon and energy balance of the overall system are evaluated as key performance indicators, based on the mass and energy flows obtained from the steady-state flowsheet model and the pinch analysis.

2.3.1. Carbon efficiency

Carbon efficiency is used as an indicator of the material-based efficiency of the overall process, as it quantifies how much of the input carbon is retained in the desired fuel products or side products rather than being lost in waste streams. This is particularly relevant for biomass-based processes, where the limited availability of biogenic feedstock makes efficient carbon utilization essential for maximizing the sustainable fuel yield per unit of biomass. The carbon efficiency is calculated according to Eq. (3). $\eta_{c,i}$ is the carbon efficiency and $\dot{n}_{c,i}$ the molar carbon flow.

$$\eta_{c,i} = \frac{\dot{n}_{c,i}}{\sum \dot{n}_{c,Feed}} \tag{3}$$

2.3.2. Energy efficiency

Energy efficiency is used as a key indicator to quantify the energetic performance of the overall process, relating the energy content of the fuel product to the energy supplied to the system. Here, the chemical energy of all mass or molar streams is expressed as higher heating value (HHV) used in the efficiency calculation to ensure a consistent energy basis.

As input energy to the overall system, the higher heating value of the feed streams, the external electricity demand, and the net external heat demand after heat integration are considered. Accordingly, the energy efficiency for each (intermediate) product can be calculated using Eq. (4). $\eta_{E,i}$ is the energy efficiency, $\dot{m}_i$ the mass flow, HHV_i the higher heating value, P_{el} the external electricity demand, and $\dot{Q}$ the external heating demand.

$$\eta_{E,i} = \frac{\dot{m}_i \, HHV_i}{\sum (\dot{m}_{Feed} \, HHV_{Feed}) + P_{el} + \dot{Q}} \tag{4}$$

3. Results and discussion

Below, the results of the overall process simulation are presented and discussed. First, the carbon balance is shown, illustrating the carbon distribution of each material stream relative to the overall carbon contained within the feed material streams. Next, the energy balance is presented, displaying all energy flows relative to the total energy input. Finally, a sensitivity analysis is elaborated with respect to the overall carbon efficiency toward the kerosene fraction.

3.1. Carbon efficiency

The carbon efficiency of the overall process is shown in Fig. 5. The subprocesses (i.e., bioconversion, catalytic hydrothermal gasification, and thermochemical conversion) are separated from each other by dashed lines and marked in the Sankey diagram (Fig. 5). The carbon feed primarily consists of food waste, accounting for 99.3% of the input carbon, with an additional 0.7% originating from the makeup extraction agent (decanol) used in the liquid-liquid extraction step.

During dark fermentation, liquid metabolites are produced containing 70.9% of the total carbon, which is further processed in the microbial electrolysis cell. Within the MEC, acetic acid is consumed, yielding a gaseous (22.9%, mainly CO_2) and a liquid intermediate-product (39.3%, containing propionic acid as the most abundant species). In the catalytic hydrothermal gasification step, all solid suspension recycling-streams (comprising microbial biomass and undigested food waste) are combined into a single feed, predominantly generating a gaseous output with minor carbon losses (3.1%) to the brine waste-stream.

In the subsequent aerobic fermentation, all gaseous intermediate-streams are merged with the liquid intermediate-stream originating in the microbial electrolysis cell. During this step, 50.6% of the feed carbon exit the system and proceeds to the purification unit, while the off-gas carbon mainly consists of CO_2. During purification, ca. 12% of the total carbon leaves the system via wastewater, largely as diluted organic compounds. After the final distillation column, 31.4% of the total carbon is available as 2,3-BDO, which is fed into the thermochemical conversion step, while 8.2% exits as acetoin used for energy recovery in the furnace.

After the dehydration of 2,3-BDO, about 5% of the total carbon leaves the system as organic compounds (mainly methyl ethyl ketone) dissolved in wastewater. The remaining carbon undergoes oligomerization, hydrogenation, and fractionation, resulting in an overall hydrocarbon yield of 25.8%. 9.6% of the overall carbon feed falls within the kerosene boiling range.

The Sankey diagram clearly highlights the major carbon losses within the overall process scheme. By far the largest carbon loss, ca. 46%, occurs as off-gas CO_2 following the aerobic fermentation. The high carbon losses can be attributed to elemental balance constraints of the system. Compared with the molar composition of the intermediate-product 2,3-BDO (C:O = 2.0; C:H = 0.4), the food-waste feedstock exhibits a lower C:O ratio (ca. 1.7) and a higher C:H ratio (ca. 0.6), indicating an over-supply of oxygen and an under-supply of hydrogen. This imbalance is further intensified by the oxygen supplied during aerobic fermentation. The consequence is that this excess oxygen needs to be removed to provide the desired intermediate and final products primarily as CO_2 and H_2O; this necessity results in substantial carbon losses in form of CO_2. Potentially, this CO_2 being of biogenic origin might serve as a feedstock for various downstream applications, including power-to-kerosene pathways when combined with additional hydrogen provided

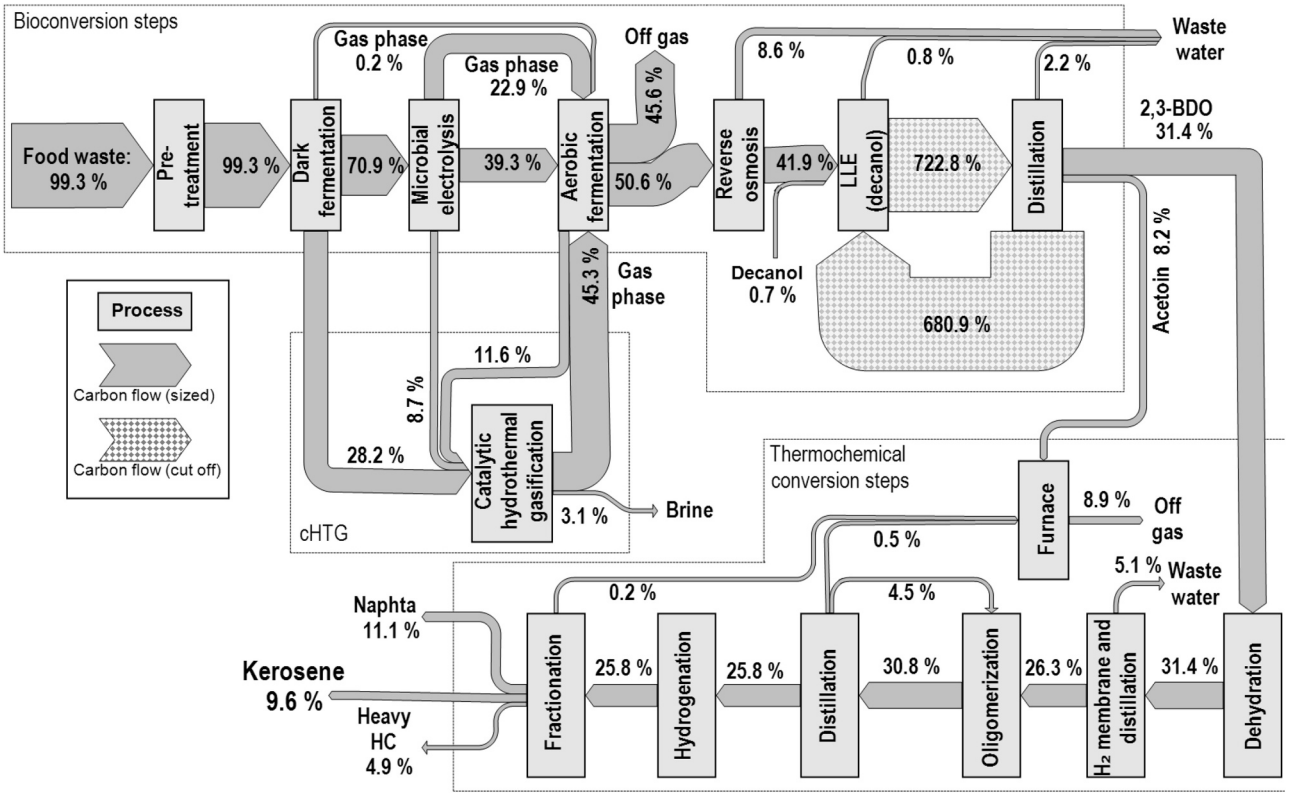


Fig. 5. Carbon flow efficiency (cHTG Catalytic hydrothermal gasification; LLE Liquid-liquid extraction; HC Hydrocarbons).

by an electrolysis with water and electricity from renewable sources of energy. But such processes are beyond the scope of this process and thus not investigated here.

Wastewater from purification offers recycling potential. Portions could be redirected to the beginning of the overall process while reducing fresh water demand. Reverse osmosis permeate is particularly promising, as organics are highly diluted, minimizing purge needs to prevent inhibitor build-up. However, as no recycling has been taken into account within the process investigated here, carbon losses in the waste water from the purification stage amount to ca. 12%.

The brine stream being another "waste stream" could potentially be valorised as a kind of fertilizer (currently under investigation), but its carbon content (accounting for ca. 3%) must still be accounted for as a conversion loss.

The modelled 2,3-BDO-to-hydrocarbon conversion exceeds 80% efficiency. Major losses arise as co-products (mainly methyl ethyl ketone (2-butanone)) from dehydration, exiting diluted in wastewater.

Although the chemical energy contained in the process streams redirected to the furnace can be recovered within the process boundaries by converting it to thermal energy through complete oxidation (Section 3.2), the associated carbon leaves the system in the form of CO_2. This waste-stream accounts for ca. 9% of the total carbon output of the process.

The oligomerization step predominantly yields C_8, C_{12}, and C_{16} olefins from the main olefin monomer in the feedstock (C_4, butene) in descending order ($C_8 > C_{12} > C_{16}$), as lower oligomers (i.e., dimers) form in higher amounts than higher ones (i.e., trimers, tetramers) according to the Anderson–Schulz–Flory distribution. Consequently, to meet the kerosene boiling range defined within the respective ASTM standard, much C_8 is directed to naphtha (44% of total hydrocarbons) and C_{16} to heavy hydrocarbons (19%), leaving 37% of the hydrocarbon carbons to the kerosene fraction (9.6% total carbon efficiency).

3.2. Energy efficiency

The energy balance can be illustrated as a Sankey diagram shown in Fig. 6. As in the carbon flow diagram (Fig. 5), the different process sections are separated by dashed lines. Each energy stream is expressed as a percentage relative to the total input energy consisting of the chemical energy of the feed streams, the electrical energy input, and the thermal energy input. External heat demand above 250 °C is supplied electrically, while heat below this temperature is provided by high-pressure steam.

The thermal energy demand is determined after internal heat integration. Cooling streams available within the process and above a certain temperature level (i.e., the heat streams from the bioconversion steps at 35 °C were not included) are considered potential heat sources, with feasible heat recovery determined by the pinch analysis (see Supplementary information – Table S11). Only the remaining heat demand is externally supplied, either as steam or electricity. This distinction between internally recovered heat and externally supplied energy is illustrated in the Sankey diagram of energy flows in Fig. 6. The central heat integration bus combines all integrated thermal energy streams, while external heating duty and cooling demand are shown separately entering or leaving the system on the right-hand side of the heat integration bus.

As in the carbon balance, the main feedstock is food waste, contributing with 60% of the total energy input. An additional 4.5% originates from auxiliary streams, including hydrogen used in the thermochemical process steps, make-up decanol as an extraction agent in the liquid-liquid extraction, and nutrients (modelled as NH_3) in the bioprocess steps. Furthermore, 15% of the total energy input is supplied as electrical energy and 20.7% as thermal energy. Of the total input, 13.8% corresponds to heat above 250 °C supplied by electricity from renewable sources of energy.

From a product perspective, the process converts 20.5% of the overall energy input into hydrocarbons, with the kerosene fraction

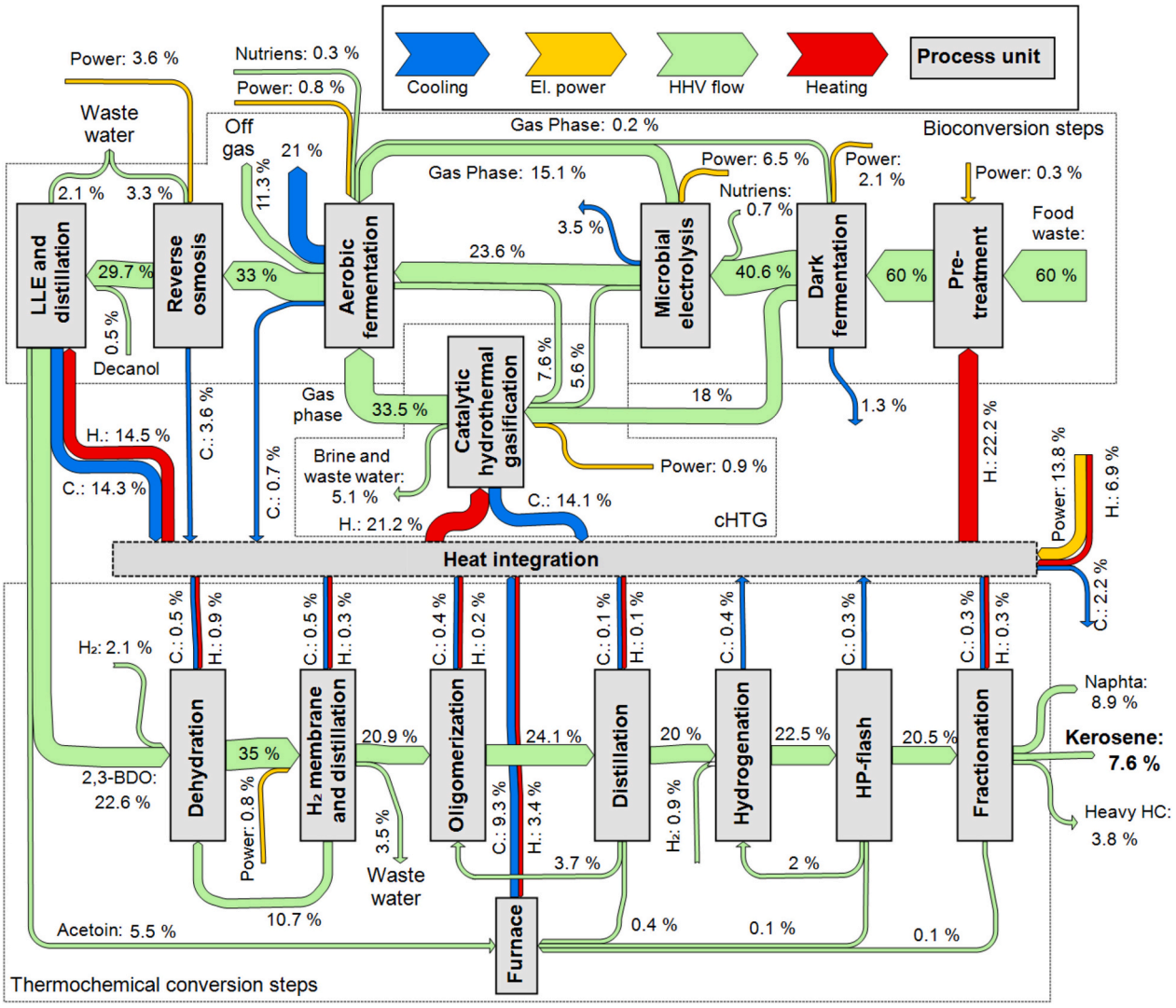


Fig. 6. Energy flow efficiencies.

representing 7.6% of the total input. The largest energy loss occurs during the aerobic fermentation stage in the form of non-recoverable (low temperature) heat. Heat released within this and other biochemical conversion steps is not considered recoverable within the heat integration analysis, as it is provided at a fairly low temperature level of ca. 35 °C. Depending on ambient conditions, additional heat losses occur in the bioreactors; i.e., most of this heat is used only to maintain a constant operating temperature. The total energy output does not sum up to 100%, as part of the heat is utilized within the system boundaries for heating duties. This is due to the assumption that all incoming material streams enter at 20 °C and all outgoing streams leave the system at 35 °C (described in the Supplementary Information).

The overall energy balance of the integrated process reveals several hotspots and inefficiencies that clearly influence the overall system performance. The pre-treatment stage is characterized by a significant heat demand resulting mainly from the high dilution of the feedstock food waste with water (i.e., ca. 0.8 wt% volatile solids [67]) assumed here. The resulting large input material stream consisting mainly of water required for feed preparation must be heated up from ambient temperature (assumed with 20 °C) to the reactor operating temperature (35 °C); this results in a considerable thermal energy input already at this very early process stage. Additionally, the pre-treatment and dark fermentation units are characterized by considerable electrical power requirements due to food waste size reduction and centrifugation operations.

The inclusion of a MEC further increases the system's electrical energy demand, accounting for ca. 6.5% of the total energy input.

Significant chemical energy losses also occur in the aqueous and brine waste-streams, corresponding to ca. 5.1% of the overall input energy. These losses primarily originate from residual organic compounds in the brine and dissolved ammonia in the wastewater resulting from nitrogen conversion and ammonia formation in the catalytic hydrothermal gasification process. Although this unit exhibits a high degree of internal heat recovery, its thermal energy demand remains the second highest in the overall conversion system. This is mainly due to the operation at elevated temperatures, reaching up to 420 °C inside the reactor.

During aerobic fermentation, additional chemical energy is lost via off-gas, mainly due to incomplete hydrogen utilization. This highlights the importance of a highly efficient autotrophic conversion route and a near-complete hydrogen conversion (further investigated in Section 3.3.2). Combustion of the off-gas is not considered here, as a more promising approach involves its material reuse within the system by adjusting the hydrogen conversion ratio. Complete hydrogen conversion would result in an off-gas with a high CO_2 molar purity of ca. 80% (Section 3.3.2), while containing only negligible amounts of combustible species such as CH_4 from the catalytic hydrothermal gasification step, and thus a marginal remaining energy content.

Further energy penalties arise from high-pressure operation in the reverse osmosis unit (up to 70 bar) and the substantial thermal load of the distillation network, particularly within the decanol recovery column. The overall process exhibits a chemical energy loss of around 5.4% due to these separation steps.

In contrast, the thermochemical subprocesses demonstrate relatively high energetic efficiency. Roughly 72% of the input energy to this subsystem can be recovered as hydrocarbons, excluding the furnace stage.

3.3. Sensitive parameters

To assess the impact of uncertainties and evaluate the robustness of the results, three process steps – microbial electrolysis cell, aerobic fermentation, and olefin oligomerization - are investigated in detail based on a sensitivity analysis. These steps are selected for distinct reasons.

- The electricity demand of the microbial electrolysis cell accounts for 6.5% of the total energy demand, making it the second largest electricity input stream, surpassed only by the electricity required for high-temperature external heat supply.
- Aerobic fermentation is associated with the largest carbon losses within the overall process (ca. 46%) and therefore represents a key leverage point for improving the overall carbon efficiency.
- The oligomerization step significantly influences the chain length distribution of the final hydrocarbon products. As such, it directly determines the yield of the kerosene fraction and consequently affects the yields of side-products (i.e., naphtha and heavy hydrocarbons).

For each investigated process step, the selected parameters were systematically varied by up to ±100% within the simulation, and the model was re-run to quantify the resulting changes in carbon efficiency toward kerosene at each variation point.

- For the microbial electrolysis cell, the conversion of acetic acid and the hydrogen recovery rate are identified as the most influential parameters and are therefore subjected to detailed sensitivity analysis. The acetic acid conversion rate (baseline: 0.8) is varied across a wide range from −100% (no conversion, acetic acid conversion rate equals 0) to +25% (complete conversion, acetic acid conversion rate equals 1.0), using increments of 10%. This range captures the full spectrum of potential process performance, from total failure of the conversion step to complete conversion. The hydrogen recovery rate, with a baseline value of 0.7, is adjusted from −100% (no hydrogen recovery, hydrogen recovery rate of 0) to +43% (maximum theoretical recovery, hydrogen recovery rate of 1.0). These variations, applied in 10% steps, illustrate the overall system's sensitivity to microbial electrolysis cell management.
- In the heterotrophic stage of the aerobic fermenter, parameter variations focused on the intermediate-product yields of 2,3-BDO, acetoin, and microbial biomass. Two distinct aspects are considered: overall microbial growth and the intermediate-product distribution between 2,3-BDO and acetoin at a fixed microbial growth rate. The latter has been analysed by the variation of the share of 2,3-BDO among the intermediate-products with a baseline value of 0.53. The maximum variation (+89%) corresponds to complete selectivity toward 2,3-BDO (i.e., share of 2,3-BDO 1.0), while the minimum (−100%) reflects exclusive acetoin formation (i.e., share of 2,3-BDO 0). The overall microbial growth has been investigated by adjusting the individual growth for each organic acid by ±100%. As all organic acids have an individual baseline growth rate (0.36 for acetic acid, 0.12 for propionic acid, 0.69 for butyric acid, and 0.74 for valeric acid), at +100%, these growth rates were doubled (i.e., acetic acid 0.72, propionic acid 0.24, butyric acid 1.00, valeric acid 1.00), while at −100%, microbial growth was set to zero for all involved volatile fatty acids. In the autotrophic stage of the aerobic fermenter, the hydrogen consumption rate (initially set to 0.8) is varied in an additional sensitivity analysis from complete inhibition of the autotrophic pathway (−100%; i.e., no hydrogen uptake, hydrogen consumption 0) to full utilization reflecting the maximum autotrophic productivity (+25%; i.e., hydrogen consumption 1.0).
- For the oligomerization step, the influence of the chain-growth probability factor on the overall process performance is investigated alongside the impact of the C_2 to C_6 olefine conversion rate. In the baseline scenario, the chain-growth probability factor has been set to 0.375, corresponding to the maximum kerosene selectivity and is varied by ±50% (i.e., in the range of 0.188 to 0.563). The impact of the C_2 to C_6 olefine conversion rate (baseline value: 0.95) has been analysed by parameter variation from −50% (corresponding to a conversion rate 0.475) up to complete conversion (i.e., conversion rate of 1.00), corresponding to an increase of ca. +5%.

The results of the sensitivity analysis are presented and discussed below, beginning with the microbial electrolysis cell, followed by the aerobic fermentation reactor, and concluding with the oligomerization parameters.

3.3.1. Microbial electrolysis cell

Fig. 7 (left) shows the results of the variations defined above; each cross represents the outcome of an individual simulation run, corresponding to a specific parameter variation from its baseline value.

- The variation of the acetic acid conversion rate is depicted with blue crosses. The resulting kerosene efficiency with changing acetic acid conversion rate remains constant across all simulations, with slight deviations (±0.06%).
- The hydrogen recovery rate is marked using green crosses. Here, only a very small variation of the overall carbon efficiency toward kerosene (i.e., 9.4% at minimum and 9.7% at maximum) can be observed, with a linear behaviour.

Changes in kerosene efficiency are marginal for both parameters analysed. The hydrogen recovery rate behaves as expected: as recovery decreases, losses to microbial biomass increase, thereby reducing overall kerosene carbon efficiency, while higher recovery improves it. Although being a loss to the microbial electrolysis cell, the carbon inside the microbial biomass is not lost to the overall system as it can be recovered in the catalytic hydrothermal gasification step. This explains the flat gradient of the curve.

The almost constant kerosene carbon efficiency with the variation of the acetic acid conversion rate indicates that acetic acid removal via the microbial electrolysis cell (together with its associated hydrogen production) is less beneficial to the overall carbon efficiency than initially anticipated. Aerobic bacteria (*C.nec.*) are capable of converting acetic acid with a decent efficiency, while simultaneously generating substantial hydrogen losses through the autotrophic pathway due to the formation of water inside the metabolic pathway. Consequently, from a carbon efficiency perspective, the inclusion of a microbial electrolysis cell in the overall process scheme appears highly questionable, as it delivers no identifiable improvement.

3.3.2. Aerobic fermenter

The results of the variation of key parameters in the aerobic fermentation are shown in Fig. 7 (right). Again, each cross represents an individual simulation run, with increments of 10% applied to each parameter.

- The hydrogen consumption (depicted as a blue line) exhibits a linear positive correlation with the overall process efficiency toward kerosene.

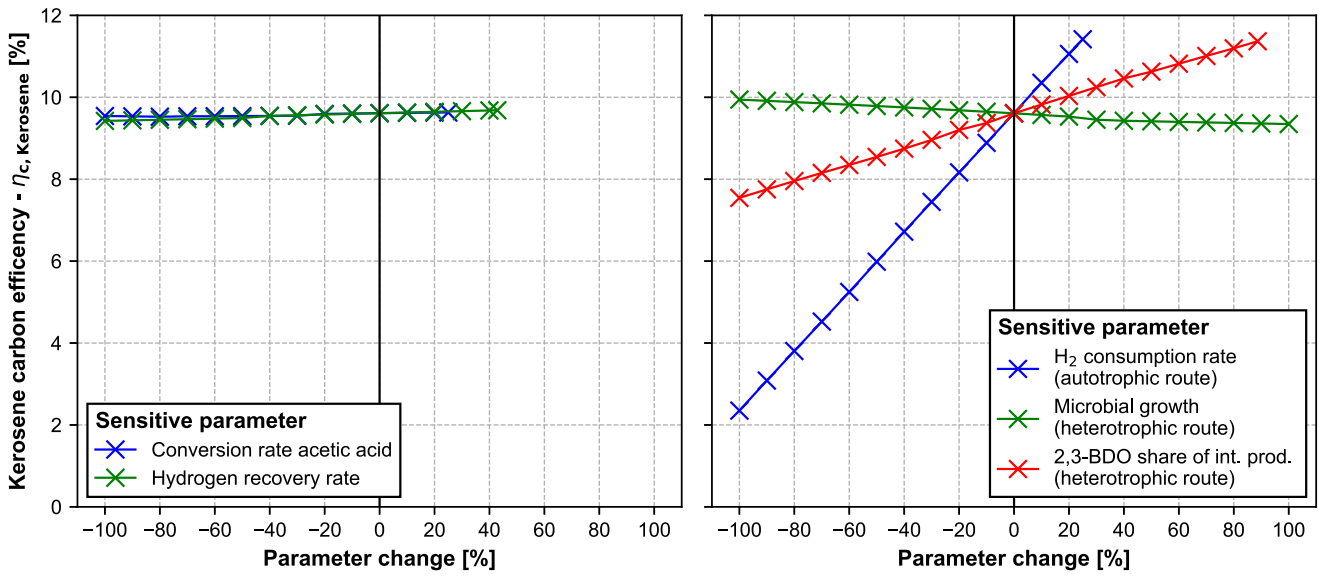


Fig. 7. Sensitivity analysis of the microbial electrolysis cell parameters (left side) and the aerobic fermentation parameters (right side; int. prod.: intermediate products).

- In the heterotrophic pathway, two parameters are examined.
  The first, shown as a red line, represents the share of 2,3-BDO among the intermediate-products (i.e., 2,3-BDO and acetoin) and again follows a positive linear trend. The second heterotrophic parameter, shown in green, represents microbial growth and thus quantifies the carbon losses during aerobic fermentation.

As expected, increasing microbial growth leads to reduced overall process efficiency, whereas lower growth improves kerosene yield. The nonlinearity of this curve arises from the distinct baseline growth rates assigned to individual volatile fatty acids and the individual variation of these growth rates. Consequently, as butyric and valeric acid reach their maximum microbial growth rates at ca. +45% and +35%, respectively, the slope of the green line begins to flatten slightly.

According to Fig. 7 (right), the hydrogen consumption rate of the autotrophic metabolic pathway has the greatest influence on kerosene yield during aerobic fermentation of the parameters examined. This aligns with the Sankey diagram showing the carbon efficiency. Here, ca. 36% of the carbon entering the aerobic fermentation originates from the liquid phase (i.e., the feedstock for the heterotrophic route) while the remaining 64% is supplied via the gas phase. Consequently, changes in the autotrophic route efficiency have a significant impact on the 2,3-BDO yield, which directly affects the overall kerosene productivity. Under conditions of complete hydrogen consumption, kerosene efficiency reaches 11.4%, while off-gas losses decrease from 45.6 to 36.1%. The resulting gas waste-stream exhibits a molar CO_2 purity above 80%, presenting an attractive point source for biogenic CO_2 recovery.

Within the heterotrophic pathway, the most significant parameter is the selectivity toward 2,3-BDO. Since the baseline selectivity between 2,3-BDO and acetoin is roughly 53:47, an increase in 2,3-BDO selectivity substantially enhances process productivity related to the kerosene fraction. Acetoin, in contrast, is not utilized as feedstock for the thermochemical conversion step and contributes only to internal energy recovery within the process. At full selectivity toward 2,3-BDO, the overall process efficiency toward kerosene increases to 11.4%.

Microbial growth shows a comparatively smaller influence on process efficiency. This is because biomass formation does not constitute a complete carbon loss; its carbon content can be recovered through gasification and subsequently reintroduced into the autotrophic route of the aerobic fermentation as CO_2.

3.3.3. *Oligomerization*

The influence of the investigated parameters in the oligomerization step is shown in Fig. 8. The variation of the chain-growth probability factor (α) is indicated in blue. In addition to the efficiency toward kerosene, the corresponding efficiencies for naphtha and heavy hydrocarbons (indicated by a dotted line with circular markers and a dashed line with square markers, respectively) are also displayed to illustrate the effect of the chain-growth probability on the distribution of hydrocarbon fractions. Each set of vertically aligned blue markers corresponds to a single simulation run, performed at a 10% parameter increment. The influence of the chain-growth probability factor on the kerosene fraction follows a parabolic trend, reaching its maximum at the baseline scenario. In contrast, the naphtha and heavy hydrocarbon fractions show decreasing and increasing trends, respectively, with rising chain-growth probabilities.

Additionally, the results of the sensitivity analysis of the olefin conversion rate are presented in red and follows an almost linear trend, with a relatively small slope, resulting in a carbon efficiency decrease of only 1.1%-points at a conversion rate of 0.475 (−50%).

The behaviour of the overall conversion system with the variation of the chain-growth probability factor (α) is consistent with the expectation that higher chain-growth probabilities favour the formation of larger olefins, thereby increasing the share of heavier hydrocarbons. Although kerosene is not the most dominant fraction at its maximum, it remains optimal at a chain-growth probability of 0.375. Notably, at a chain-growth probability value between 0.45 and 0.5, the kerosene fraction becomes the most abundant, but since this point does not coincide with the peak of the curve, it is not considered the preferred operating condition. Due to the parabolic nature of the kerosene curve, variations of the chain-growth probability within ±20% have only a minor effect on kerosene efficiency, resulting in a decrease of ca. 0.2% kerosene efficiency.

The oligomerization rate behaves as expected; with a higher conversion rate of the feed olefins (C_2 to C_6), more kerosene is produced, and vice versa. The relatively small slope of the linear trend can be explained by the recycling of unconverted olefins. However, since the purge rate of the recycle-stream is fixed at 10%, lower conversion rates result in a larger total recycle flow, which in turn increases the stream directed from the oligomerization step to thermal energy recovery in the furnace.

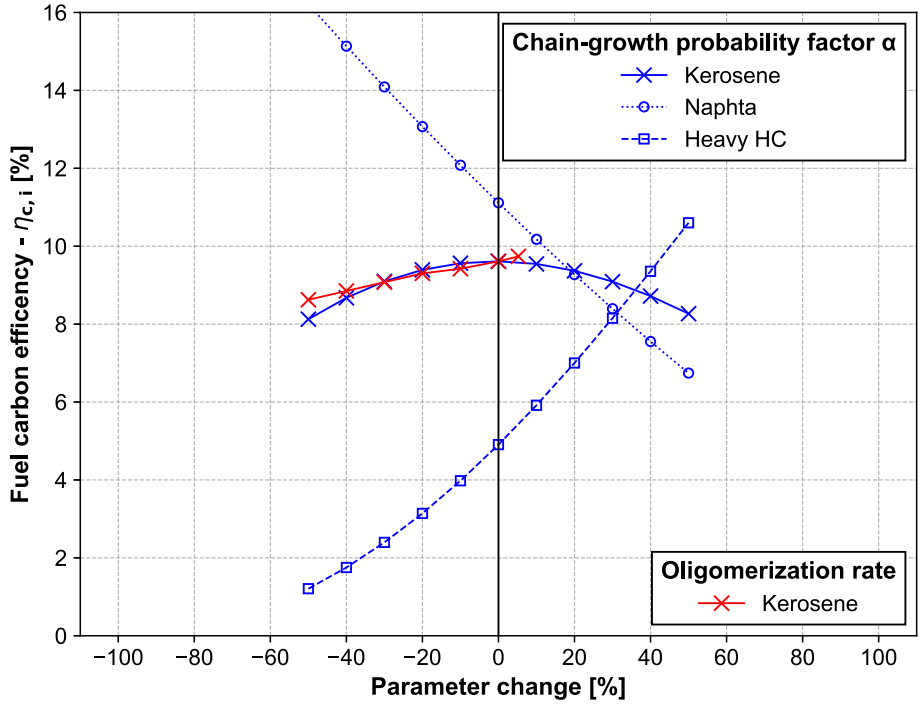


Fig. 8. Sensitivity analysis of oligomerization parameters (HC: hydrocarbon).

3.4. Final process assessment and perspectives

Achieving the climate targets of the aviation sector requires large-scale production and usage of sustainable aviation fuels as an essential step toward net-zero greenhouse gas emissions. However, the currently dominant SAF production route HEFA faces limited scalability due to considerable constraints related to the demanded lipid-based feedstock (vegetable oil and used cooking oils). This highlights the need to explore alternative, feedstock-diverse production pathways. The present analysis focuses on carbon and energy efficiency as key performance indicators to evaluate the potential of the proposed SAF production pathway and to identify opportunities for further improvement. For context, carbon efficiencies of other biomass based SAF production pathways (an alcohol-to-jet study and a gasification-based Fischer-Tropsch (FT) study) are briefly summarized, while noting that a direct comparison with the food-waste-to-2,3-BDO-to-jet-fuel pathway is not meaningful at this stage due to fundamental differences in system boundaries and assumptions.

- Alcohol-to-jet. A recent study investigated two pathways using corn stover as the main carbon source: (1) ethanol fermentation followed by an alcohol-to-jet conversion, and (2) anaerobic digestion, followed by a methanol synthesis and a methanol-to-jet route. The reported carbon efficiencies to kerosene lie between 19% and 23%. A direct comparison is questionable because primary feedstock is corn stover rather than food waste, and the digestate that is not utilized within the system boundaries except for heat integration in some scenarios [82].
- Fischer-Tropsch: A forest-residue-to-Fischer-Tropsch-liquid study reports carbon efficiencies of 34–61% toward hydrocarbons higher than C_5, highly depending on the process configuration and, in particular, on the inclusion of electrolysis and thus non biomass derived hydrogen. Comparability to the present process is highly limited: dry forest-residue chips were the primary biomass, and depending on the scenario, either no CO_2 and no additional hydrogen were considered, or CO2 was recycled and additional hydrogen was supplied via electrolysis to adjust the H2/CO2 ratio. In contrast, the here investigated concept introduces hydrogen only in the thermochemical conversion subprocess. Additional differences arise as in the FT-process no heat integration is performed and all alkanes with a carbon number higher than C5 are viewed as products [83].

Energy efficiencies are not compared because of even more fundamental methodological differences, such as the use of lower heating value versus higher heating value as basis for calculation and different heat integration assumptions. As illustrated, any direct numerical comparison of carbon and energy efficiencies across pathways is highly sensitive to methodological choices and may be misleading unless conducted on the basis of fully harmonized assumptions and system boundaries.

The current study was therefore designed to assess the proposed pathway, highlighting achievable conversion efficiencies while simultaneously identifying routes for further improvement, and thereby forming the basis for a subsequent analysis. A key finding is that the anticipated improvements in carbon yield through the introduction of a microbial electrolysis cell were not achieved. By simulating a wide range of different MEC productivity scenarios, including complete MEC failure (no acetic acid conversion, i.e., a simulation run without any MEC conversion), the results indicate that the MEC inclusion is unnecessary, as same kerosene yields can be achieved without it. This has a direct impact on the economic analysis, as the process becomes less complex, requiring less equipment while simultaneously reducing electricity demand (6.5% of the overall input energy is consumed by the MEC), thereby directly lowering utility costs. Given that the MEC does not improve carbon yields and that the process configuration can be simplified accordingly, the next critical question concerns the feasibility of the streamlined process at pilot and industrial scale.

Challenges are expected when scaling up the reactors to the dimensions considered for the pilot and, subsequently, a large-scale plant operating in long-term continuous mode, which may significantly affect the overall economic feasibility. Particular attention must be paid to membrane fouling control in the filtration stages downstream of the bioreactors as well as in the reverse osmosis unit. In addition, catalyst lifetime studies are required to enable a robust assessment of catalyst replacement demands over the plant lifetime. These scale-up and

durability aspects should be explicitly addressed in a subsequent economic analysis, in which appropriate metrics are applied to capture uncertainties in component lifetimes and associated replacement costs.

4. Conclusion

The present study conducts a technical assessment of a novel SAF production pathway using food waste as the primary feedstock, 2,3-butanediol (2,3-BDO) as a key intermediate-product, and integrates biogenic as well as thermochemical conversion processes, providing a quantitative basis for further process development. Based on the methodological framework, the main results of the analysis can be summarized as follows.

- Carbon efficiency. The carbon efficiency analysis revealed the conversion of the feed carbon through multiple process stages, with major losses occurring mainly as gaseous CO_2 and diluted organic compounds in wastewater. Starting from food waste as the dominant carbon source, the biochemical conversion steps, supported by the catalytic hydrothermal gasification unit, converted ca. 50% of the input carbon into intermediate liquid products, with 2,3-BDO as the main compound and acetoin as main co-product, which is used for energy recovery. After the purification of the 2,3-BDO produced, roughly 31% of the total carbon were transferred to the thermochemical conversion section in the form of purified 2,3-BDO. Despite partial losses in subsequent thermochemical conversion and purification steps, the integrated process achieved an overall hydrocarbon yield of about 25%, of which about 10% falls within the kerosene boiling range.
- Energy efficiency. The energy balance evaluation illustrated the distribution of the total input across the process steps, revealing that the most significant energy losses occur during the biochemical conversion stages. Starting from food waste as the main energy carrier, supported by auxiliary inputs such as electricity, hydrogen, and thermal energy, ca. 20% of the total input energy is recovered as hydrocarbons, with about 8% corresponding to the kerosene fraction. The largest irrecoverable losses are associated with aerobic fermentation, where low temperature heat is dissipated and cannot be utilized for process integration. Chemical energy losses are primarily associated with hydrogen losses during the aerobic fermentation stage, amounting to about 11%, as well as with compounds diluted in the wastewater streams, which accounts for roughly 14% throughout the entire process.

Based on a sensitivity analysis, key parameters for potential process improvement are identified. The use of a microbial electrolysis cell does not appear to contribute positively to the overall carbon conversion efficiency and is associated with a high electrical energy demand reducing the overall energy efficiency. Therefore, the use of a microbial electrolysis cell should be excluded from further process optimization studies. The autotrophic stage has been identified as the main leverage point for improving carbon efficiency. With a maximum hydrogen conversion rate, the carbon efficiency toward the kerosene fraction could be increased by up to 2%-points. In contrast, a reduction in hydrogen conversion efficiency would have a major impact, potentially decreasing the kerosene fraction to below 3% in the most extreme case.

Additionally, the results for energy efficiency clearly reveal the high thermal energy demand of the pre-treatment stage. Therefore, the dark fermentation step should be further investigated with regard to reducing the water demand and, consequently, the dilution of the food waste used as a feedstock. Lower water content would reduce the overall energetic burden and allow for smaller reactor volumes, which is particularly relevant when considering the economic feasibility of the process.

In future studies, a focus should additionally be placed on implementing improvement measures and on exploring potential utilization options of co-products such as acetoin and CO_2. The use of acetoin as an additional feedstock for the dehydration stage within the thermochemical conversion sequence, or its direct conversion into hydrocarbon fractions within the jet-fuel range, could offer promising carbon yield improvement options. Furthermore, purification and reuse of CO_2 as a feedstock in power-to-liquid applications may represent an interesting option for enhancing overall carbon utilization. Finally, a comparison with alternative bio-thermochemical conversion routes should be carried out under consistent system boundary conditions to identify the most effective strategy for valorising food waste, a currently abundant yet underutilized biogenic resource.

CRediT authorship contribution statement

Felix Mendler: Writing – original draft, Software, Methodology, Investigation, Formal analysis, Conceptualization. **Steffen Voß:** Validation, Software, Methodology. **Martin Kaltschmitt:** Writing – review & editing, Supervision, Conceptualization.

Declaration of generative AI and AI-assisted technologies in the writing process

During the preparation of this work, the authors used Perplexity AI and OpenAI's ChatGPT in order to improve the readability and language clarity of the manuscript. After using these tools, the authors reviewed and edited the content as needed and take full responsibility for the content of the published article.

Declaration of competing interest

The authors declare that they have no known competing financial interests or personal relationships that could have appeared to influence the work reported in this paper.

Acknowledgment

The authors acknowledge the financial support of BIOCTANE Project with Grant N° 101084336. Funded by the European Union. Views and opinions expressed are however those of the author(s) only and do not necessarily reflect those of the European Union or the European Climate, Infrastructure and Environment Agency (CINEA). Neither the European Union nor CINEA can be held responsible for them.

The authors gratefully acknowledge INRAE LBE, Narbonne, France for hosting F. Mendler for a one-week research visit and for numerous valuable discussions that supported this work.

Appendix A. Supplementary data

Supplementary data to this article can be found online at https://doi.org/10.1016/j.fuproc.2026.108630.

Data availability

Data will be made available on request.

References

[1] Ipcc, Global Warming of 1.5 °C: IPCC Special Report on Impacts of Global Warming of 1.5 °C above Pre-Industrial Levels in Context of Strengthening Response to Climate Change, Sustainable Development, and Efforts to Eradicate Poverty, 1st ed, Cambridge University Press, 2022, https://doi.org/10.1017/9781009157940.
[2] E. Graham, N. Fulghum, Global Electricity Review 2025, Ember, London, 2025.
[3] Defossilising Aviation With e-SAF – An Introduction to Technologies, Policies, and Markets for Sustainable Aviation Fuels, Agora Verkehrswende and PtX Hub, 2024.
[4] O. Rosales Calderon, L. Tao, Z. Abdullah, K. Moriarty, S. Smolinski, A. Milbrandt, et al., Sustainable Aviation Fuel (SAF) State-of-Industry Report: State of SAF Production Process, 2024, https://doi.org/10.2172/2426562.
[5] Specification for Aviation Turbine Fuel Containing Synthesized Hydrocarbons, ASTM International, West Conshohocken, PA, 2021, https://doi.org/10.1520/D7566-21.

[6] Global Feedstock Assessment for SAF Production - Outlook to 2050, IATA, 2025.
[7] Publications Office of the European Union, RefuelEU Aviation – Sustainable Air Transport, 2024.
[8] S. Scherhaufer, G. Moates, H. Hartikainen, K. Waldron, G. Obersteiner, Environmental impacts of food waste in Europe, Waste Manag. 77 (2018) 98–113, https://doi.org/10.1016/j.wasman.2018.04.038.
[9] Eurostat, Food Waste and Food Waste Prevention by NACE Rev. 2 Activity - Tonnes of Fresh Mass, 2024, https://doi.org/10.2908/ENV_WASFW.
[10] S.P. Adhikari, J. Zhang, Q. Guo, K.A. Unocic, L. Tao, Z. Li, A hybrid pathway to biojet fuel *via* 2,3-butanediol, Sustainable Energy Fuels 4 (2020) 3904–3914, https://doi.org/10.1039/D0SE00480D.
[11] C.W. Song, J.M. Park, S.C. Chung, S.Y. Lee, H. Song, Microbial production of 2,3-butanediol for industrial applications, J. Ind. Microbiol. Biotechnol. 46 (2019) 1583–1601, https://doi.org/10.1007/s10295-019-02231-0.
[12] D. Härrer, C. Windhorst, N. Böhner, J. Novion Ducassou, Y. Couté, J. Gescher, Production of acetoin from renewable resources under heterotrophic and mixotrophic conditions, Bioresour. Technol. 329 (2021) 124866, https://doi.org/10.1016/j.biortech.2021.124866.
[13] M. Weldon, C. Euler, Physiology-informed use of Cupriavidus necator in biomanufacturing: a review of advances and challenges, Microb. Cell Factories 24 (2025) 30, https://doi.org/10.1186/s12934-025-02643-x.
[14] J.R. Weiler, N. Jürgensen, M. Cornejo Infante, M.T. Knoll, J. Gescher, Strain and model development for auto- and heterotrophic 2,3-butanediol production using Cupriavidus necator H16, Biotechnol. Biofuels Bioprod. 17 (2024) 108, https://doi.org/10.1186/s13068-024-02549-7.
[15] M. Kaltschmitt, H. Hofbauer, V. Lenz (Eds.), Energie aus Biomasse: Thermochemische Konversion, Springer Fachmedien Wiesbaden, Wiesbaden, 2024, https://doi.org/10.1007/978-3-658-41216-6.
[16] F. Vogel, T. Brunner, D. Baudouin, R. Zambrano, G. Peng, A. Mian, et al., HydroPilot: Pilot Plant for the Catalytic Hydrothermal Gasification of Wet Biomass, Paul Scherrer Institut (PSI), Bern, 2023.
[17] D.J.M. De Vlieger, A.G. Chakinala, L. Lefferts, S.R.A. Kersten, K. Seshan, D.W. F. Brilman, Hydrogen from ethylene glycol by supercritical water reforming using noble and base metal catalysts, Appl. Catal. B Environ. 111–112 (2012) 536–544, https://doi.org/10.1016/j.apcatb.2011.11.005.
[18] B.R. Tiwari, S.K. Maity, S.K. Brar, K.W. Chew, G. Kumar, V. Kumar, Comprehensive techno-economic and environmental assessment for 2,3-butanediol production from bread waste, Chem. Eng. J. 500 (2024) 157003, https://doi.org/10.1016/j.cej.2024.157003.
[19] F.B. Lueckel, F. Scott, G. Aroca, Comparative techno-economic and carbon footprint analysis of 2,3-butanediol production through aerobic and anaerobic bioconversion of carbon dioxide with green hydrogen, Chem. Eng. J. Adv. 20 (2024) 100659, https://doi.org/10.1016/j.ceja.2024.100659.
[20] M. Affandy, C. Zhu, M. Swita, B. Hofstad, D. Cronin, R. Elander, et al., Production and catalytic upgrading of 2,3-butanediol fermentation broth into sustainable aviation fuel blendstock and fuel properties measurement, Fuel 333 (2023) 126328, https://doi.org/10.1016/j.fuel.2022.126328.
[21] M.J. Cordon, H. Olcay, P.G.N. Neate, M.K. Kidder, A. Lawal, M. Li, et al., Cost-effective valorization of 2,3-butanediol to high-value chemicals and jet fuel, Joule (2026) 102536, https://doi.org/10.1016/j.joule.2026.102536.
[22] C. Banks, S. Heaven, Y. Zhang, U. Baier, Food Waste Digestion: Anaerobic Digestion of Food Waste for a Circular Economy, IEA Bioenergy, 2018.
[23] Y.M. Gu, S.Y. Park, J.Y. Park, B.-I. Sang, B.S. Jeon, H. Kim, et al., Impact of attrition ball-mill on characteristics and biochemical methane potential of food waste, Energies 14 (2021) 2085, https://doi.org/10.3390/en14082085.
[24] S. Panigrahi, B.K. Dubey, A critical review on operating parameters and strategies to improve the biogas yield from anaerobic digestion of organic fraction of municipal solid waste, Renew. Energy 143 (2019) 779–797, https://doi.org/10.1016/j.renene.2019.05.040.
[25] F.O. Agyeman, W. Tao, Anaerobic co-digestion of food waste and dairy manure: effects of food waste particle size and organic loading rate, J. Environ. Manag. 133 (2014) 268–274, https://doi.org/10.1016/j.jenvman.2013.12.016.
[26] M. Gallego-García, A.D. Moreno, P. Manzanares, M.J. Negro, A. Duque, Recent advances on physical technologies for the pretreatment of food waste and lignocellulosic residues, Bioresour. Technol. 369 (2023) 128397, https://doi.org/10.1016/j.biortech.2022.128397.
[27] K. Lehmphul, Biogasanlagen, Umweltbundesamt, 2015. https://www.umweltbundesamt.de/themen/wirtschaft-konsum/industriebranchen/biogasanlagen (accessed January 29, 2025).
[28] Q. Wang, H. Li, K. Feng, J. Liu, Oriented fermentation of food waste towards high-value products: a review, Energies 13 (2020) 5638, https://doi.org/10.3390/en13215638.
[29] G.M. Teke, B. Anye Cho, C.E. Bosman, Z. Mapholi, D. Zhang, R.W.M. Pott, Towards industrial biological hydrogen production: a review, World J. Microbiol. Biotechnol. 40 (2024) 37, https://doi.org/10.1007/s11274-023-03845-4.
[30] Y. Chen, X. Zhang, Y. Chen, Propionic acid-rich fermentation (PARF) production from organic wastes: a review, Bioresour. Technol. 339 (2021) 125569, https://doi.org/10.1016/j.biortech.2021.125569.
[31] E. Howley, D. Ki, R. Krajmalnik-Brown, C.I. Torres, *Geobacter sulfurreducens*' unique metabolism results in cells with a high iron and lipid content, Microbiol. Spectrum 10 (2022) e02593-22, https://doi.org/10.1128/spectrum.02593-22.
[32] J.A. Magdalena, M.F. Pérez-Bernal, N. Bernet, E. Trably, Sequential dark fermentation and microbial electrolysis cells for hydrogen production: volatile fatty acids influence and energy considerations, Bioresour. Technol. 374 (2023) 128803, https://doi.org/10.1016/j.biortech.2023.128803.
[33] A. Kadier, Y. Simayi, P. Abdeshahian, N.F. Azman, K. Chandrasekhar, M.S. Kalil, A comprehensive review of microbial electrolysis cells (MEC) reactor designs and configurations for sustainable hydrogen gas production, Alex. Eng. J. 55 (2016) 427–443, https://doi.org/10.1016/j.aej.2015.10.008.
[34] R. Rousseau, L. Etcheverry, E. Roubaud, R. Basséguy, M.-L. Délia, A. Bergel, Microbial electrolysis cell (MEC): strengths, weaknesses and research needs from electrochemical engineering standpoint, Appl. Energy 257 (2020) 113938, https://doi.org/10.1016/j.apenergy.2019.113938.
[35] R. Nerenberg, The membrane-biofilm reactor (MBfR) as a counter-diffusional biofilm process, Curr. Opin. Biotechnol. 38 (2016) 131–136, https://doi.org/10.1016/j.copbio.2016.01.015.
[36] S.C. Lee, H.C. Woo, Y.H. Kim, Energy-efficient recovery process of 2,3-butanediol using 2-heptanol extraction, Chem. Eng. Process. Process Intensif. 160 (2021) 108286, https://doi.org/10.1016/j.cep.2020.108286.
[37] P.M. Gawal, Cost-effective 2,3-BD separation: insights from aqueous two-phase extraction-assisted distillation, Biomass Convers. Biorefinery (2024), https://doi.org/10.1007/s13399-024-05392-w.
[38] B.N. Trusty, S. Dangwal, Z. Coin, S. Pramanik, R. Bhave, S.Z. Islam, 2,3-Butanediol recovery from fermentation broth using membrane pertraction, Chem. Eng. Process. Process Intensif. 219 (2026) 110579, https://doi.org/10.1016/j.cep.2025.110579.
[39] D. Baudouin, D. Salionov, F. Vogel, S. Bjelić, Advanced analytical study of process streams for a rational optimization of hydrothermal gasification, ACS Eng. Au 1 (2021) 134–147, https://doi.org/10.1021/acsengineeringau.1c00010.
[40] A. Hartwig, MAK Commission, Kerosin (Erdöl), MAK-Begründung, 2020, https://doi.org/10.34865/MB800820D5_2OR.
[41] M.A. Lilga, G.-S. Lee, S.-J. Lee, USO09517984B2: Conversion of 2,3-Butanediol to 2-Butanol, Olefins and Fuels, 2016.
[42] S. Adhikari, J. Zhang, K. Unocic, E.C. Wegener, P. Kunal, D.J. Deka, et al., Direct 2,3-butanediol conversion to butene-rich C_{3+} olefins over copper-modified 2D pillared MFI: consequence of reduced diffusion length, ACS Sustain. Chem. Eng. 10 (2022) 1664–1674, https://doi.org/10.1021/acssuschemeng.1c07670.
[43] B.A. Bekele, J. Poissonnier, J.W. Thybaut, The potential of ZrO2 catalysts for the dehydration of 2,3-butanediol into 3-buten-2-ol: Impact of synthesis method and operating conditions, J. Catal. 411 (2022) 200–211, https://doi.org/10.1016/j.jcat.2022.05.011.
[44] I. Lemir, A. Souza, S. Turriziani, M. del Mar Alonso-Doncel, D. Serrano, P. Pizarro, Tailoring the Cu/ZSM-5 Catalyst Properties for Effective Conversion of Bioderived 2,3-Butanediol Into Butenes, Internal BIOCTANE project data; manuscript under publication process. Once published, it will be listed on the BIOCTANE website, https://www.bioctane.eu/research/, 2026.
[45] B.H. Babu, M. Lee, D.W. Hwang, Y. Kim, H.-J. Chae, An integrated process for production of jet-fuel range olefins from ethylene using Ni-AlSBA-15 and Amberlyst-35 catalysts, Appl. Catal. A Gen. 530 (2017) 48–55, https://doi.org/10.1016/j.apcata.2016.11.020.
[46] J. Smith, M. Sjodin, P. Starkey, S. Donen, M. Shebowich, US11078433: Conversion of Mixtures of c2 – c8, Olefins to Jet Fuel and/or Diesel Fuel in High Yield From Bio-Based Alcohols, 2021.
[47] M.A. Lilga, R.T. Hallen, K.O. Albrecht, A.R. Cooper, J.G. Frye, K.K. Ramasamy, US20170218283A1: Systems and Processes for Conversion of Ethylene Feedstocks to Hydrocarbon Fuels, 2017.
[48] M. Díaz, E. Epelde, Z. Tabernilla, A. Ateka, A.T. Aguayo, J. Bilbao, Operating conditions to maximize clean liquid fuels yield by oligomerization of 1-butene on HZSM-5 zeolite catalysts, Energy 207 (2020) 118317, https://doi.org/10.1016/j.energy.2020.118317.
[49] A.F. Silva, P. Neves, S.M. Rocha, C.M. Silva, A.A. Valente, Optimization of continuous-flow heterogeneous catalytic oligomerization of 1-butene by design of experiments and response surface methodology, Fuel 259 (2020) 116256, https://doi.org/10.1016/j.fuel.2019.116256.
[50] N.M. Eagan, M.D. Kumbhalkar, J.S. Buchanan, J.A. Dumesic, G.W. Huber, Chemistries and processes for the conversion of ethanol into middle-distillate fuels, Nat. Rev. Chem. 3 (2019) 223–249, https://doi.org/10.1038/s41570-019-0084-4.
[51] D. Schröder, Herstellung kurz- und mittelkettiger Olefine durch Fischer-Tropsch-Synthese, . Dissertation,, Universität Bayreuth, 2022.
[52] F. Pöhlmann, Zusammenspiel von chemischer Reaktion und Porendiffusion bei der kobaltkatalysierten Fischer-Tropsch-Synthese unter Einsatz von CO2-haltigem Synthesegas, Dissertation, Universität Bayreuth, 2017.
[53] S. Bube, N. Bullerdiek, S. Voß, M. Kaltschmitt, Kerosene production from power-based syngas – a technical comparison of the Fischer-Tropsch and methanol pathway, Fuel 366 (2024) 131269, https://doi.org/10.1016/j.fuel.2024.131269.
[54] G.J.P. Britovsek, R. Malinowski, D.S. McGuinness, J.D. Nobbs, A.K. Tomov, A. W. Wadsley, et al., Ethylene oligomerization beyond Schulz–Flory distributions, ACS Catal. 5 (2015) 6922–6925, https://doi.org/10.1021/acscatal.5b02203.
[55] M.A. Fahim, T.A. Alsahhaf, A. Elkilani, Hydroconversion, in: Fundam. Pet. Refin., Elsevier, 2010, pp. 153–198, https://doi.org/10.1016/B978-0-444-52785-1.00007-3.
[56] L. Tao, J.N. Markham, Z. Haq, M.J. Biddy, Techno-economic analysis for upgrading the biomass-derived ethanol-to-jet blendstocks, Green Chem. 19 (2017) 1082–1101, https://doi.org/10.1039/C6GC02800D.
[57] S. Geleynse, K. Brandt, M. Garcia-Perez, M. Wolcott, X. Zhang, The alcohol-to-jet conversion pathway for drop-in biofuels: techno-economic evaluation, ChemSusChem 11 (2018) 3728–3741, https://doi.org/10.1002/cssc.201801690.
[58] AspenTech, Aspen Plus - The Leading Process Simulation Software in the Chemical Industry. https://www.aspentech.com/en/products/engineering/aspen-plus, 2026 (n.d., accessed March 16, 2026).
[59] Aspen Technology, Aspen Energy Analyzer - Reference Guide, 2011.

[60] J. Schermuly, S. Walk, I. Körner, A.E. Arroyo Cuara, V. Oyedele, S. Deegener, Report on results for household food waste collection and decentralised shredding in the "Lübeck-case": DECISIVE Deliverable D3.6 : a decentralised management scheme for innovative valorisation of urban biowaste, 2018, https://doi.org/10.15480/882.1706.
[61] I. Angelidaki, L. Ellegaard, B.K. Ahring, A comprehensive model of anaerobic bioconversion of complex substrates to biogas, Biotechnol. Bioeng. 63 (1999) 363–372, https://doi.org/10.1002/(SICI)1097-0290(19990505)63:3%3C363::AID-BIT13%3E3.0.CO;2-Z.
[62] I. Angelidaki, L. Ellegaard, B.K. Ahring, A mathematical model for dynamic simulation of anaerobic digestion of complex substrates: focusing on ammonia inhibition, Biotechnol. Bioeng. 42 (1993) 159–166, https://doi.org/10.1002/bit.260420203.
[63] D.J. Batstone, J. Keller, I. Angelidaki, S.V. Kalyuzhnyi, S.G. Pavlostathis, A. Rozzi, et al., The IWA anaerobic digestion model no 1 (ADM1), Water Sci. Technol. (2002) 65–73.
[64] K. Rajendran, H.R. Kankanala, M. Lundin, M.J. Taherzadeh, A novel process simulation model (PSM) for anaerobic digestion using Aspen Plus, Bioresour. Technol. 168 (2014) 7–13, https://doi.org/10.1016/j.biortech.2014.01.051.
[65] V. Gadhamshetty, Y. Arudchelvam, N. Nirmalakhandan, D.C. Johnson, Modeling dark fermentation for biohydrogen production: ADM1-based model vs. Gompertz model, Int. J. Hydrog. Energy 35 (2010) 479–490, https://doi.org/10.1016/j.ijhydene.2009.11.007.
[66] M. Alexandropoulou, G. Antonopoulou, G. Lyberatos, A novel approach of modeling continuous dark hydrogen fermentation, Bioresour. Technol. 250 (2018) 784–792, https://doi.org/10.1016/j.biortech.2017.12.005.
[67] M. Bourgeois, S. Taussac, N. Bernet, R. Escudié, E. Trably, Effect of operating conditions on food waste fermentation to enhance VFA production and propionic acid selectivity, Environ. Technol. Innov. 39 (2025) 104324, https://doi.org/10.1016/j.eti.2025.104324.
[68] R. Moletta, Dynamic modelling of anaerobic digestion, Water Res. 20 (1986) 427–434, https://doi.org/10.1016/0043-1354(86)90189-2.
[69] G. Mohanakrishna, N.P. Sneha, S.M. Rafi, O. Sarkar, Dark fermentative hydrogen production: potential of food waste as future energy needs, Sci. Total Environ. 888 (2023) 163801, https://doi.org/10.1016/j.scitotenv.2023.163801.
[70] P.J. Weimer, M. Nerdahl, D.J. Brandl, Production of medium-chain volatile fatty acids by mixed ruminal microorganisms is enhanced by ethanol in co-culture with Clostridium kluyveri, Bioresour. Technol. 175 (2015) 97–101, https://doi.org/10.1016/j.biortech.2014.10.054.
[71] R.P. Pinto, B. Srinivasan, A. Escapa, B. Tartakovsky, Multi-population model of a microbial electrolysis cell, Environ. Sci. Technol. 45 (2011) 5039–5046, https://doi.org/10.1021/es104268g.
[72] P. Kurzweil, Brennstoffzellentechnik, Springer Fachmedien Wiesbaden, Wiesbaden, 2016, https://doi.org/10.1007/978-3-658-14935-2.
[73] R. Moscoviz, J. Toledo-Alarcón, E. Trably, N. Bernet, Electro-fermentation: how to drive fermentation using electrochemical systems, Trends Biotechnol. 34 (2016) 856–865, https://doi.org/10.1016/j.tibtech.2016.04.009.
[74] A. Buttler, H. Spliethoff, Current status of water electrolysis for energy storage, grid balancing and sector coupling via power-to-gas and power-to-liquids: a review, Renew. Sust. Energ. Rev. 82 (2018) 2440–2454, https://doi.org/10.1016/j.rser.2017.09.003.
[75] E. Trably, J.A. Magdalena, M.F. Pérez-Bernal, N. Bernet, Microbial Electrolysis Cells as a Tool to Polish Short Chain -Rich Dark Fermentation Effluents for Propionate Production, 2024, https://doi.org/10.2139/ssrn.5041100.
[76] D.F. Call, R.C. Wagner, B.E. Logan, Hydrogen production by *Geobacter* species and a mixed consortium in a microbial electrolysis cell, Appl. Environ. Microbiol. 75 (2009) 7579–7587, https://doi.org/10.1128/AEM.01760-09.
[77] J. Han, W. Liu, T. Zhang, K. Xue, W. Li, F. Jiao, et al., Mechanism study on the sulfidation of ZnO with sulfur and iron oxide at high temperature, Sci. Rep. 7 (2017) 42536, https://doi.org/10.1038/srep42536.
[78] K. Khandelwal, P. Boahene, S. Nanda, A.K. Dalai, A review of the design and performance of catalysts for hydrothermal gasification of biomass to produce hydrogen-rich gas fuel, Molecules 28 (2023) 5137, https://doi.org/10.3390/molecules28135137.
[79] F. Moradi Estalkhzir, H. Ramezanipour Penchah, H. Ghanadzadeh Gilani, H. Mikayilzadeh, Experimental data of citric acid extraction from aqueous solution with 1-decanol by using liquid–liquid equilibrium, J. Chem. Eng. Data 63 (2018) 3227–3236, https://doi.org/10.1021/acs.jced.7b01135.
[80] W.-W. Seo, J.-H. Yim, J.S. Lim, K.Y. Choi, Liquid-liquid equilibrium (LLE) data of ternary mixtures of [water+acetic acid+1-nonanol] and [water+acetic acid+1-decanol] at 298.2–318.2 K and 101.3 kPa, Korean J. Chem. Eng. 39 (2022) 3422–3433, https://doi.org/10.1007/s11814-022-1196-y.
[81] C.J. Davey, A. Havill, D. Leak, D.A. Patterson, Nanofiltration and reverse osmosis membranes for purification and concentration of a 2,3-butanediol producing gas fermentation broth, J. Membr. Sci. 518 (2016) 150–158, https://doi.org/10.1016/j.memsci.2016.06.044.
[82] S. Voß, S. Bube, M. Kaltschmitt, Aviation fuel production pathways from lignocellulosic biomass via alcohol intermediates – a technical analysis, Fuel Commun. 17 (2023) 100093, https://doi.org/10.1016/j.jfueco.2023.100093.
[83] F. Habermeyer, E. Kurkela, S. Maier, R.-U. Dietrich, Techno-economic analysis of a flexible process concept for the production of transport fuels and heat from biomass and renewable electricity, Front. Energy Res. 9 (2021) 723774, https://doi.org/10.3389/fenrg.2021.723774.